

Journal of
Mechanics of
Materials and Structures

**TWO-WAY THERMOMECHANICALLY COUPLED
MICROMECHANICAL ANALYSIS OF SHAPE MEMORY ALLOY
COMPOSITES**

Jacob Aboudi and Yuval Freed

Volume 1, N° 5

May 2006

 mathematical sciences publishers

TWO-WAY THERMOMECHANICALLY COUPLED MICROMECHANICAL ANALYSIS OF SHAPE MEMORY ALLOY COMPOSITES

JACOB ABOUDI AND YUVAL FREED

A previously established micromechanical model whose capability to analyze and predict the behavior of thermoelastic fibrous composites with one-way thermomechanical coupling, in which the temperature is prescribed in advance, was verified. This model is extended herein to incorporate two-way thermomechanical coupling effects in thermoelastic composites. As a result of this generalization, the temperature which is coupled to the mechanical effects, is governed by the energy equation and is induced into the composite's constituents as a result of the application of mechanical loadings. The model is applied to predict the behavior of composites that consist of shape memory alloy fibers embedded in metallic and polymeric matrices. Results exhibit the response of the composites to various types of loading, and the effect of the two-way thermomechanical coupling that induces temperature deviations from reference temperatures at which shape memory and pseudoelasticity effects take place at the fibers.

1. Introduction

Shape memory alloy (SMA) materials undergo phase transformation which is caused by the application of stress and/or change in temperature. At high temperatures, the material behavior is nonlinear and hysteretic, but, at the end of a mechanical loading-unloading cycle, still yields the original stress-strain-free state (pseudoelastic behavior). At lower temperatures, a mechanical loading-unloading results in a residual deformation which can be recovered by a temperature increase (shape memory effect). The latter effect can be utilized to control the behavior of structures in which SMA materials have been embedded.

There are numerous micromechanical models that can predict the overall (macroscopic) behavior of composite materials with embedded shape memory alloy fibers. Examples for such micromechanical investigations are those of [Boyd and Lagoudas \[1994\]](#), [Kawai et al. \[1999\]](#), [Carvelli and Taliercio \[1999\]](#), [Song et al. \[1999\]](#), [Kawai \[2000\]](#), [Gilat and Aboudi \[2004\]](#) and [Marfia \[2005\]](#). When thermal effects in these investigations are involved, they are treated as in thermal stress problems where a prescribed constant temperature is imposed throughout the composite. The thermomechanical coupling (TMC) in such thermoelastic problems is referred to as one-way coupling because only the mechanical field is affected by the temperature. A micro-macro-structural analysis with one-way TMC was recently employed by [Gilat and Aboudi \[2006\]](#) to investigate the thermal buckling of shape memory reinforced laminated plates.

In thermomechanical problems with two-way TMC, the temperature and mechanical effects are coupled to each other and the energy equation that governs the temperature field variation in the material involves the effect of total strain rate, the effect of inelastic strain rate in metallic materials and the effect

Keywords: shape memory alloys, periodic composites, thermomechanical coupling, micromechanics, high-fidelity generalized method of cells.

of transformation strain rate in SMA materials. In order to investigate the behavior of the monolithic SMA material with two-way TMC, appropriate constitutive relations and the energy equation need to be established. To this end, [Auricchio and Petrini \[2004b\]](#) presented a free-energy function from which the required two-way TMC constitutive and energy equations were derived. The implementation of these equations requires the development of a computational algorithm based on an implicit time procedure, in conjunction with the radial return method [\[Simo and Hughes 1998\]](#).

The purpose of the present paper is two-fold. First, a micromechanical model, referred to as a *high-fidelity generalized method of cells* (HFGMC) is generalized to incorporate two-way TMC capability. The HFGMC with one-way coupling can predict the behavior of multiphase inelastic composites with periodic microstructure by employing the homogenization technique. Its accuracy and reliability were demonstrated [\[Aboudi et al. 2002; 2003\]](#) by comparisons with analytical solutions that can be established in certain cases and with finite element solutions. The method has been employed also for the prediction of the behavior of viscoelastic-viscoplastic composites [\[Aboudi 2005\]](#), electro-magneto-thermoelastic composites, and composites that are subjected to large deformations, see the recent review by [Aboudi \[2004\]](#) (that includes also references to its predecessor GMC micromechanical model). It should be noted that the HFGMC with one-way TMC has been implemented in the recently developed micromechanics analysis code MAC/GMC by NASA Glenn Research Center, which has many user friendly features and significant flexibility; see [\[Bednarczyk and Arnold 2002\]](#) for the most recent version of its user guides. The predecessor GMC micromechanical model was employed by [Williams and Aboudi \[1999\]](#) to investigate two-way TMC of metal matrix composites.

As a result of the generalization offered by the HFGMC to incorporate the two-way TMC, macroscopic constitutive equations that govern the thermomechanical behavior of the composite are established. These relations are based on the micromechanical derivation of the effective stiffness tensor of the composite as well as the mechanical, thermal and inelastic concentration tensors and scalars. These concentration tensors and scalars are established by the homogenization of the periodic composite, in conjunction with the imposition of the coupled equilibrium and energy equations, and by imposing the continuity of tractions, displacements, heat fluxes and temperatures at the interfaces between the various materials, and by the application of the periodic boundary conditions. The latter conditions ensure that the tractions, displacements, heat fluxes and temperatures are identical at the opposite boundaries of a repeating unit cell that characterizes the periodic composite. These three types of concentration tensors are interrelated due to the TMC effects. In particular, the effective stiffness tensor of the composite involves the mechanical and thermal concentration tensors.

The second purpose of this paper is the investigation of the overall (macroscopic) behavior of composites consisting of continuous SMA fibers embedded in metallic and polymeric matrices with two-way TMC effects. In particular, the induced average temperatures that result from the two-way TMC are computed and presented under various circumstances. To this end, the constitutive two-way modeling of the SMA fibers of [Auricchio and Petrini \[2004b\]](#) is employed.

Results are given for SMA continuous fiber composites with a metallic (aluminum) matrix and polymeric (epoxy) matrix. It is shown that the TMC has little effect on the average stress-strain of the composite, but has a significant effect on the induced temperature that is generated due to the application of mechanical loadings. This effect is due mainly to the term that appears in the coupled energy equation that involves the inelastic strain rate in metallic materials, and to a lesser extent, to the transformation

strain rate in the SMA fibers. These results are given at two reference temperatures at which shape memory and pseudoelasticity effects in the SMA fibers take place.

2. Two-way TMC constitutive equations of the monolithic SMA

The fully coupled thermomechanical equations of the monolithic SMA material were presented by Auricchio and Petri [2002; 2004b; 2004a], who extended and improved the thermodynamical model of Souza et al. [1998]. These equations are briefly presented below. The strain $\boldsymbol{\epsilon}$ is decoupled into a dilatation θ and deviatoric \mathbf{e} parts as follows:

$$\boldsymbol{\epsilon} = \frac{\theta}{3}\mathbf{I} + \mathbf{e}, \quad (1)$$

where \mathbf{I} is the unit tensor. The free energy function ψ is a function of the dilatation strain θ , the deviatoric strain \mathbf{e} , the transformation strain \mathbf{e}^{tr} and absolute temperature T , given by

$$\begin{aligned} \rho\psi(\theta, \mathbf{e}, \mathbf{e}^{tr}, T) = & \frac{1}{2}K\theta^2 + G\|\mathbf{e} - \mathbf{e}^{tr}\|^2 - 3\alpha K\theta(T - T_0) + \beta \langle T - M_f \rangle \|\mathbf{e}^{tr}\| \\ & + \frac{h}{2}\|\mathbf{e}^{tr}\|^2 + (u_0 - T\eta_0) + \rho c_v \left[T - T_0 - T \log \frac{T}{T_0} \right] + \Upsilon(\mathbf{e}^{tr}), \quad (2) \end{aligned}$$

where ρ , K , G , α , T_0 , β , M_f , h , and ρc_v are the mass density, bulk modulus, shear modulus, coefficient of thermal expansion, reference temperature, slope of the stress-temperature relation, martensite final temperature, slope of the stress-strain relation during the stress-induced phase transformation and the heat capacity, respectively. In addition, u_0 and η_0 are the internal energy and entropy at the reference state. In Equation (2), $\|\cdot\|$ and $\langle \cdot \rangle$ denote the Euclidean norm and the positive part of the argument respectively, and $\Upsilon(\mathbf{e}^{tr})$ is an indicator function defined as

$$\Upsilon(\mathbf{e}^{tr}) = \begin{cases} 0 & \|\mathbf{e}^{tr}\| \leq \epsilon_L, \\ \infty & \|\mathbf{e}^{tr}\| > \epsilon_L, \end{cases}$$

where ϵ_L is the norm of the maximum transformation strain reached at the end of the transformation during uniaxial test.

The resulting constitutive relations obtained from Equation (2) are given by

$$\begin{aligned} p &= \frac{\partial \psi}{\partial \theta} = K[\theta - 3\alpha(T - T_0)], \\ \mathbf{s} &= \frac{\partial \psi}{\partial \mathbf{e}} = 2G(\mathbf{e} - \mathbf{e}^{tr}), \\ \eta &= -\frac{\partial \psi}{\partial T} = \eta_0 + 3K\alpha\theta - \beta\|\mathbf{e}^{tr}\| \frac{\langle T - M_f \rangle}{|T - M_f|} + \rho c_v \log \frac{T}{T_0}, \\ \mathbf{X} &= -\frac{\partial \psi}{\partial \mathbf{e}^{tr}} = \mathbf{s} - \left[\beta(T - M_f) + h\|\mathbf{e}^{tr}\| + \frac{\partial \Upsilon(\mathbf{e}^{tr})}{\partial \|\mathbf{e}^{tr}\|} \right] \frac{\partial \|\mathbf{e}^{tr}\|}{\partial \mathbf{e}^{tr}}, \end{aligned}$$

where p and \mathbf{s} are the volumetric and deviatoric parts of the stress $\boldsymbol{\sigma}$, η is the entropy and \mathbf{X} is the transformation stress associated with \mathbf{e}^{tr} .

The evolution law of \mathbf{e}^{tr} is

$$\dot{\mathbf{e}}^{tr} = \dot{\zeta} \frac{\partial F(\mathbf{X})}{\partial \boldsymbol{\sigma}} \quad (3)$$

where the dot denotes a derivative with respect to time t , and F and $\dot{\zeta}$ play the roles of limit function and plastic consistent parameter, subject to the Kuhn–Tucker conditions. For symmetric SMA behavior, the function F is given by

$$F(\mathbf{X}) = \|\mathbf{X}\| - R \leq 0, \quad (4)$$

where R is the radius of the elastic domain.

The resulting coupled energy equation is given by

$$\rho c_v \dot{T} + \nabla \cdot \mathbf{q} = \left[\mathbf{X} + T\beta \frac{\mathbf{e}^{tr}}{\|\mathbf{e}^{tr}\|} \right] : \dot{\mathbf{e}}^{tr} - 3 T K \alpha \dot{\theta}, \quad (5)$$

in conjunction with the Fourier law that relates the heat flux \mathbf{q} to the temperature gradient:

$$\mathbf{q} = -k \nabla T, \quad (6)$$

with k being the heat conductivity.

The above nonlinear equations have been treated by Auricchio and Petrini [2002; 2004b; 2004a] who employed for their solution a computational algorithm based on an implicit time procedure. This algorithm consists of integrating these equations over a time interval $[t_n, t_{n+1}]$ using an implicit backward Euler scheme. Thus, assuming the knowledge of the solution at time t_n , as well as the strain $\boldsymbol{\epsilon}$ at time t_{n+1} , the stresses are computed using the radial return mapping algorithm [Simo and Hughes 1998].

It should be noted that in the case of standard isotropic materials (for example, metallic materials) the energy equation is of a form similar to Equation (5) [Allen 1991], but with the term

$$\left[\mathbf{X} + T\beta \frac{\mathbf{e}^{tr}}{\|\mathbf{e}^{tr}\|} \right] : \dot{\mathbf{e}}^{tr}$$

replaced by the rate of inelastic work: $\dot{W}_I = \boldsymbol{\sigma} : \dot{\boldsymbol{\epsilon}}^I$, where $\boldsymbol{\epsilon}^I$ is the inelastic strain which replaces the transformation strain $\boldsymbol{\epsilon}^{tr}$ of the SMA material. In addition, \dot{W}_I is usually multiplied by a partition factor ζ to indicate that only a portion of the inelastic work (about 90%) is transformed into heat [Hunter 1983]. Thus, the final form of the energy equation for conventional isotropic materials is given by

$$\rho c_v \dot{T} + \nabla \cdot \mathbf{q} = \zeta \boldsymbol{\sigma} : \dot{\boldsymbol{\epsilon}}^I - 3 T K \alpha \dot{\theta}. \quad (7)$$

As it is shown in the following section, the spatial derivatives can be eliminated. As a result, Equations (5) and (7) are reduced to an ordinary differential equation in time. Consequently, let us represent (5) and (7) in the following compact form

$$[M]\dot{T} = [S]T + [\dot{Q}], \quad (8)$$

where $[\dot{Q}]$ denotes the right side of Equations (5) and (7). The implicit difference in time of Equation (8) yields [Mitchell and Griffiths 1980]

$$\left\{ [M] - \omega \Delta t [S] \right\} T^{n+1} = \left\{ [M] + (1 - \omega) \Delta t [S] \right\} T^n + [Q]^n - [Q]^{n-1}, \quad (9)$$

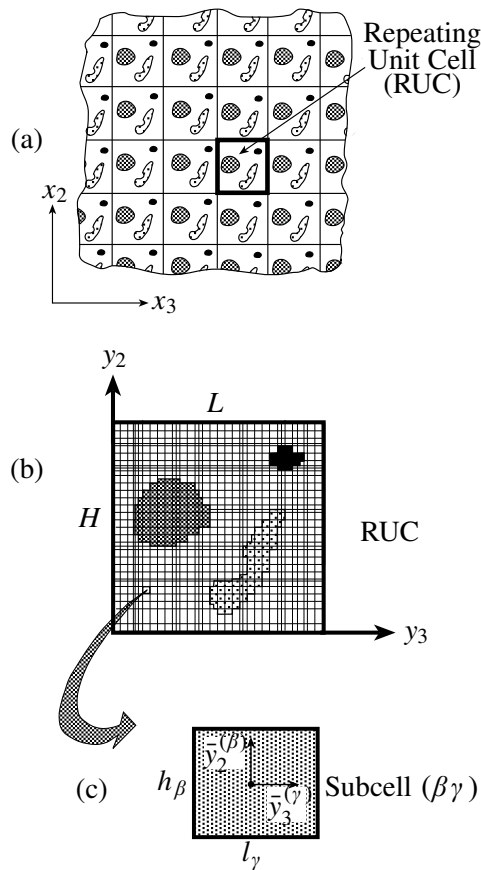


Figure 1. (a) A multiphase composite with doubly-periodic microstructures defined with respect to global coordinates (x_2, x_3) . (b) The repeating unit cell is represented with respect to local coordinates (y_2, y_3) . It is divided into N_β and N_γ subcells, in the y_2 and y_3 directions, respectively. (c) A characteristic subcell $(\beta\gamma)$ with local coordinates $\bar{y}_2^{(\beta)}$ and $\bar{y}_3^{(\gamma)}$ whose origin is located at its center.

where $\Delta t = t_{n+1} - t_n$ and ω is a parameter (for the Crank–Nicolson scheme: $\omega = 1/2$).

3. Two-way TMC micromechanical analysis

The HFGMC micromechanical model, which is extended herein to a two-way TMC, is used to predict the fully coupled thermoelastic behavior of doubly periodic composites with SMA continuous fibers. For doubly periodic elastoplastic composites with one-way TMC, this theory has been fully described by [Aboudi et al. 2002; 2003] and by [Bednarczyk et al. 2004] for elastoplastic composites with imperfect bonding between the constituents. In these publications, the reliability and accuracy of the micromechanical predictions were examined by comparisons with analytical solutions that can be established in some special cases and with a finite element procedure. In this paper, this micromechanical model with two-way TMC is briefly outlined.

This model is based on a homogenization technique for composites with periodic microstructure as shown in **Figure 1(a)** in terms of the global coordinates (x_2, x_3) . The repeating unit cell, **Figure 1(b)**, defined with respect to local coordinates (y_2, y_3) , of such a composite is divided into N_β and N_γ subcells in the y_2 and y_3 directions. Each subcell is labeled by the indices $(\beta\gamma)$ with $\beta = 1, \dots, N_\beta$ and $\gamma = 1, \dots, N_\gamma$, and may contain a distinct homogeneous material. The dimensions of subcell $(\beta\gamma)$ in the y_2 and y_3 directions are denoted by h_β and l_γ . A local coordinate system $(\bar{y}_2^{(\beta)}, \bar{y}_3^{(\gamma)})$ is introduced in each subcell whose origin is located at its center, see **Figure 1(c)**.

The local (subcell) constitutive equation of the material which, in general, is assumed to be thermoelastic is given by

$$\boldsymbol{\sigma}^{(\beta\gamma)} = \mathbf{C}^{(\beta\gamma)}(\boldsymbol{\epsilon}^{(\beta\gamma)} - \boldsymbol{\epsilon}^{I(\beta\gamma)}) - \Gamma^{(\beta\gamma)} \Delta T^{(\beta\gamma)} \tag{10}$$

where $\boldsymbol{\sigma}^{(\beta\gamma)}$, $\boldsymbol{\epsilon}^{(\beta\gamma)}$, $\boldsymbol{\epsilon}^{I(\beta\gamma)}$ and $\Gamma^{(\beta\gamma)}$ are the stress, total strain, inelastic strain and thermal stress coefficients tensors in subcell $(\beta\gamma)$. In **Equation (10)**, $\mathbf{C}^{(\beta\gamma)}$ is the stiffness tensor of the material in the subcell $(\beta\gamma)$, and $\Delta T^{(\beta\gamma)}$ denotes the temperature deviation from a reference temperature. The inelastic strain $\boldsymbol{\epsilon}^{I(\beta\gamma)}$ is governed by the flow rule (3) for SMA materials, by the Prandtl–Reuss equations of the classical plasticity or by an appropriate viscoplastic flow rule.

The basic assumption in HFGMC with one-way TMC is that the displacement vector $\mathbf{u}^{(\beta\gamma)}$ in each subcell is expanded into quadratic forms in terms of its local coordinates $(\bar{y}_2^{(\beta)}, \bar{y}_3^{(\gamma)})$, as follows

$$\begin{aligned} \mathbf{u}^{(\beta\gamma)} = & \bar{\boldsymbol{\epsilon}} \cdot \mathbf{x} + \mathbf{W}_{(00)}^{(\beta\gamma)} + \bar{y}_2^{(\beta)} \mathbf{W}_{(10)}^{(\beta\gamma)} + \bar{y}_3^{(\gamma)} \mathbf{W}_{(01)}^{(\beta\gamma)} \\ & + \frac{1}{2} \left(3\bar{y}_2^{(\beta)2} - \frac{h_\beta^2}{4} \right) \mathbf{W}_{(20)}^{(\beta\gamma)} + \frac{1}{2} \left(3\bar{y}_3^{(\gamma)2} - \frac{l_\gamma^2}{4} \right) \mathbf{W}_{(02)}^{(\beta\gamma)} \end{aligned} \tag{11}$$

where $\bar{\boldsymbol{\epsilon}}$ is the externally applied average strain, $\mathbf{W}_{(00)}^{(\beta\gamma)}$ is the volume-averaged displacement, and the higher-order terms

$$\mathbf{W}_{(mn)}^{(\beta\gamma)}$$

must be determined as discussed below.

In the two-way thermomechanically coupled HFGMC, the unknown temperature deviation $\Delta T^{(\beta\gamma)}$ in the subcell is also expanded as follows

$$\begin{aligned} \Delta T^{(\beta\gamma)} = & \Delta T_{(00)}^{(\beta\gamma)} + \bar{y}_2^{(\beta)} \Delta T_{(10)}^{(\beta\gamma)} + \bar{y}_3^{(\gamma)} \Delta T_{(01)}^{(\beta\gamma)} \\ & + \frac{1}{2} \left(3\bar{y}_2^{(\beta)2} - \frac{h_\beta^2}{4} \right) \Delta T_{(20)}^{(\beta\gamma)} + \frac{1}{2} \left(3\bar{y}_3^{(\gamma)2} - \frac{l_\gamma^2}{4} \right) \Delta T_{(02)}^{(\beta\gamma)}, \end{aligned} \tag{12}$$

where $\Delta T_{(00)}^{(\beta\gamma)}$ is the volume-averaged temperature and the higher-order terms $\Delta T_{(mn)}^{(\beta\gamma)}$ are additional unknowns.

The unknown terms

$$\mathbf{W}_{(mn)}^{(\beta\gamma)} \quad \text{and} \quad \Delta T_{(mn)}^{(\beta\gamma)}$$

are determined from the fulfillment of the coupled equilibrium and energy equations, the periodic boundary conditions, and the interfacial continuity conditions of displacements, tractions, temperatures and heat fluxes between subcells. The periodic boundary conditions ensure that the displacements, tractions, temperatures and heat fluxes at opposite surfaces of the repeating unit cell (that is, at $y_2 = 0$ and H as

well as $y_3 = 0$ and L) are identical, see [Aboudi \[2004\]](#) for more details pertaining to the micromechanical analysis with one-way TMC. A requisite in the present micromechanical analysis is that all these conditions are imposed in the average (integral) sense.

As a result of the imposition of these conditions, a linear system of algebraic equations at the current time step is obtained which can be represented in the following form

$$\mathbf{K}\mathbf{U} = \mathbf{f} + \mathbf{g}, \quad (13)$$

where the matrix \mathbf{K} contains information on the geometry and thermomechanical properties of the materials within the individual subcells ($\beta\gamma$), and the displacement-temperature vector \mathbf{U} contains the unknown displacement and temperature coefficients:

$$\mathbf{U} = [\mathbf{U}^{(11)}, \dots, \mathbf{U}^{(N_\beta N_\gamma)}], \quad (14)$$

where in subcell ($\beta\gamma$) these coefficients, which appear on the right side of Equations (11)–(12), are

$$\mathbf{U}^{(\beta\gamma)} = (\mathbf{W}_{(00)}, \Delta T_{(00)}, \mathbf{W}_{(10)}, \Delta T_{(10)}, \mathbf{W}_{(01)}, \Delta T_{(01)}, \mathbf{W}_{(20)}, \Delta T_{(20)}, \mathbf{W}_{(02)}, \Delta T_{(02)})^{(\beta\gamma)}. \quad (15)$$

The mechanical vector \mathbf{f} contains information on the applied average (far-field) strains $\bar{\boldsymbol{\epsilon}}$. The inelastic force vector \mathbf{g} appearing on the right side of [Equation \(13\)](#) contains the inelastic effects given in terms of the integrals of the inelastic strain distributions. These integrals depend implicitly on the elements of the displacement-temperature coefficient vector \mathbf{U} , requiring an incremental procedure of [Equation \(13\)](#) at each point along the loading path, see [\[Aboudi et al. 2003\]](#) for more details.

Due to the dependence of the elements of \mathbf{K} on the temperature, it is necessary to invert this matrix at every time step. The solution of [Equation \(13\)](#) at a given time step yields the following localization expression which relates the average strain $\bar{\boldsymbol{\epsilon}}^{(\beta\gamma)}$ and temperature $\Delta \bar{T}^{(\beta\gamma)}$ in the subcell ($\beta\gamma$) to the externally applied average strain $\bar{\boldsymbol{\epsilon}}$ in the form:

$$\begin{Bmatrix} \bar{\boldsymbol{\epsilon}}^{(\beta\gamma)} \\ \Delta \bar{T}^{(\beta\gamma)} \end{Bmatrix} = \begin{Bmatrix} \mathbf{A}^{M(\beta\gamma)} \\ \mathbf{A}^{T(\beta\gamma)} \end{Bmatrix} \bar{\boldsymbol{\epsilon}} + \begin{Bmatrix} \mathbf{V}^T(\beta\gamma) \\ v^T(\beta\gamma) \end{Bmatrix} + \begin{Bmatrix} \mathbf{V}^I(\beta\gamma) \\ v^I(\beta\gamma) \end{Bmatrix}, \quad (16)$$

where $\mathbf{A}^{M(\beta\gamma)}$ and $\mathbf{A}^{T(\beta\gamma)}$ are the mechanical and thermal concentration tensors of the subcell ($\beta\gamma$), $\mathbf{V}^T(\beta\gamma)$ and $\mathbf{V}^I(\beta\gamma)$ are second-order tensors that involve thermal and inelastic effects in the subcell, and $v^T(\beta\gamma)$ and $v^I(\beta\gamma)$ are the corresponding scalars. These second-order thermal and inelastic tensors and the corresponding scalars arise due to the existence of $[Q]^{n-1}$ in [Equation \(9\)](#) at the previous time step. It should be noted that in the present case of two-way TMC, the application of the far-field strain $\bar{\boldsymbol{\epsilon}}$ induces a temperature deviation from the reference temperature $\Delta T^{(\beta\gamma)}$ in the subcell.

In order to establish the global (macroscopic) constitutive equation of the composite, we use the definition of the average stress in the composite in terms of average stress in the subcells:

$$\bar{\boldsymbol{\sigma}} = \frac{1}{HL} \sum_{\beta=1}^{N_\beta} \sum_{\gamma=1}^{N_\gamma} h_\beta l_\gamma \bar{\boldsymbol{\sigma}}^{(\beta\gamma)}, \quad (17)$$

where $\bar{\boldsymbol{\sigma}}^{(\beta\gamma)}$ is the average stress in the subcell. By substituting [Equation \(10\)](#) and [\(16\)](#) into [\(17\)](#), one obtains the final form of the effective constitutive law of the multiphase fully coupled thermo-inelastic

Property	Value
E	70 GPa
ν	0.33
k	18 W/(m K)
α	$1 \times 10^{-6}/\text{K}$
ρc_v	5.44 MJ/(m ³ K)
h	500 MPa
R	45 MPa
β	7.5 MPa/K
ϵ_L	0.03
M_f	253.15 K

Table 1. Material properties of the SMA fibers [Auricchio and Petrini 2002]. E , ν denote the Young's modulus and Poisson's ratio. The other parameters were already defined in Section 2.

composite, which relates the average stress $\bar{\boldsymbol{\sigma}}$, strain $\bar{\boldsymbol{\epsilon}}$, thermal stress $\bar{\boldsymbol{\sigma}}^T$ and inelastic stress $\bar{\boldsymbol{\sigma}}^I$ as follows

$$\bar{\boldsymbol{\sigma}} = \mathbf{C}^* \bar{\boldsymbol{\epsilon}} - (\bar{\boldsymbol{\sigma}}^T + \bar{\boldsymbol{\sigma}}^I). \quad (18)$$

In this equation \mathbf{C}^* is the effective stiffness tensor which is given by

$$\mathbf{C}^* = \frac{1}{HL} \sum_{\beta=1}^{N_\beta} \sum_{\gamma=1}^{N_\gamma} h_\beta l_\gamma (\mathbf{C}^{(\beta\gamma)} \mathbf{A}^{M(\beta\gamma)} - \Gamma^{(\beta\gamma)} \mathbf{A}^{T(\beta\gamma)}). \quad (19)$$

The global thermal stress $\bar{\boldsymbol{\sigma}}^T$ is determined from

$$\bar{\boldsymbol{\sigma}}^T = -\frac{1}{HL} \sum_{\beta=1}^{N_\beta} \sum_{\gamma=1}^{N_\gamma} h_\beta l_\gamma (\mathbf{C}^{(\beta\gamma)} \mathbf{V}^{T(\beta\gamma)} - \Gamma^{(\beta\gamma)} \mathbf{v}^{T(\beta\gamma)}). \quad (20)$$

The global inelastic stress $\bar{\boldsymbol{\sigma}}^I$ is of the form

$$\bar{\boldsymbol{\sigma}}^I = -\frac{1}{HL} \sum_{\beta=1}^{N_\beta} \sum_{\gamma=1}^{N_\gamma} h_\beta l_\gamma (\mathbf{C}^{(\beta\gamma)} \mathbf{V}^{I(\beta\gamma)} - \Gamma^{(\beta\gamma)} \mathbf{v}^{I(\beta\gamma)} - \bar{\boldsymbol{\sigma}}^{I(\beta\gamma)}), \quad (21)$$

where the inelastic stress in the subcell is: $\bar{\boldsymbol{\sigma}}^{I(\beta\gamma)} = \mathbf{C}^{(\beta\gamma)} \bar{\boldsymbol{\epsilon}}^{I(\beta\gamma)}$. Finally, the global average temperature $\Delta \bar{T}$ in the composite can be determined from a simple averaging of all temperature deviations $\Delta \bar{T}^{(\beta\gamma)}$ in the subcells.

4. Applications

The established two-way TMC micromechanics is applied herein to predict the behavior of SMA composites in various circumstances. Two types of matrices are chosen to illustrate the responses of the

E (GPa)	ν	$\alpha(10^{-6}/\text{K})$	σ_y (MPa)	E_s (GPa)	k (W/(mK))	ρc_v (MJ/(m ³ K))
72.4	0.33	22.5	371.5	23	116.7	2.25

Table 2. Elastic, plastic and thermal parameters of the isotropic elastoplastic aluminum matrix. E , ν , α , σ_y , E_s , k and ρc_v denote the Young's modulus, Poisson's ratio, coefficient of thermal expansion, yield stress, secondary modulus, thermal conduction and heat capacity, respectively.

E (GPa)	ν	$\alpha(10^{-6}/\text{K})$	k (W/(mK))	ρc_v (MJ/(m ³ K))
3.45	0.35	54	0.18	1.28

Table 3. Elastic and thermal parameters of the isotropic epoxy polymeric matrix. E , ν , α , k and ρc_v denote the Young's modulus, Poisson's ratio, coefficient of thermal expansion, thermal conduction and heat capacity, respectively.

composites. In the first case an aluminum alloy is chosen as a matrix. In this case the inelasticity of the metallic matrix and its two-way TMC are involved (see Equation (7)) in addition to the two-way TMC of the SMA fibers (see Equation (5)). In the second type, a polymeric matrix (epoxy) is chosen. Here, the TMC arises due to the existence of the volumetric strain rate $\dot{\theta}$ in Equation (7) only (since $\dot{W}_I = 0$). The material properties of the SMA fibers and the aluminum and epoxy matrices are given in Tables 1–3. The present results were obtained by dividing the repeating unit cell, Figure 1(b), into $N_\beta = 3$ and $N_\gamma = 3$ subcells with the SMA fiber occupying the central subcell. In all cases the volume fraction of the SMA fibers is 0.3.

4.1. Monolithic SMA behavior. The uniaxial stress-strain behavior of the monolithic SMA fibers is shown in Figures 2 and 3 at reference temperatures $T_0 = 253.15$ K and $T_0 = 285.15$ K. At the first temperature the material is stable in the martensitic phase and the shape memory effect takes place: the mechanical loading-unloading results in a residual deformation which can be recovered by a temperature increase. At the second temperature the material is stable in the austenitic phase and the pseudoelasticity effect takes place: the material behavior is nonlinear and hysteretic but yields the original stress-strain-free state at the end of the mechanical loading-unloading. The figures show also the induced temperature deviations due to the TMC. These temperatures are caused mainly by the existence of the term

$$\left(\mathbf{X} + T\beta \frac{\mathbf{e}^{tr}}{\|\mathbf{e}^{tr}\|} \right) : \dot{\mathbf{e}}^{tr}$$

in the energy Equation (5) which is the counterpart of the rate of the inelastic work \dot{W}_I in Equation (7). Indeed, the standard thermomechanical coupling coefficient

$$\delta = \frac{E(1+\nu)\alpha^2 T_0}{(1-2\nu)(1-\nu)\rho c_v}, \quad (22)$$

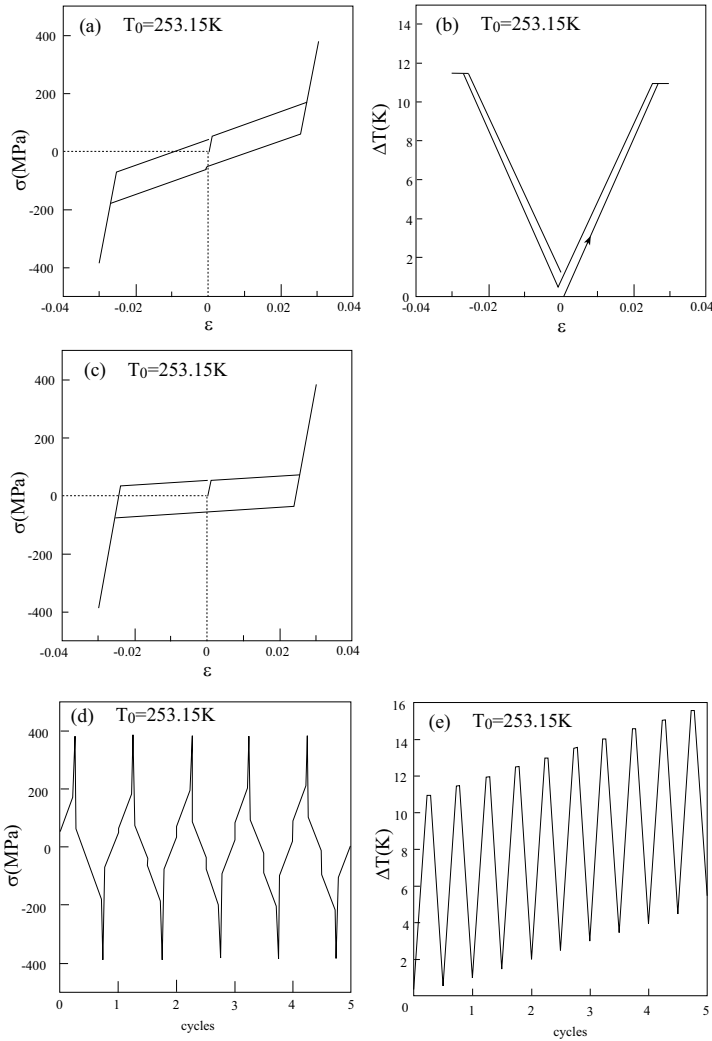


Figure 2. (a) The uniaxial stress-strain response in one cycle of SMA and, (b) the corresponding induced temperature deviation. (c) The corresponding uniaxial stress-strain response of SMA when the TMC is neglected. (d) The uniaxial stress-strain response in five cycles of SMA and (e) the corresponding induced temperature deviation. In all cases the reference temperature is $T_0 = 253.15$ K.

that characterizes the amount of coupling in thermoelastic material (that is, the coupling that is caused by the term $3 T K \alpha \dot{\theta}$ in Equation (5)) is equal to 0.2×10^{-4} for the considered SMA material, which is very small. The rate effects in the present SMA material are negligibly small. Figures 2(c) and 3(c) (which coincide with those given by Auricchio and Petrini [2002]) show the SMA response at these reference temperatures when the TMC is neglected. It is well observed that the effect of TMC on the SMA behavior is significant. This is reflected in the change of the stress-strain slope when the phase transformation takes place due to the induced temperature changes. Figures 2(b) and 3(b) show that there

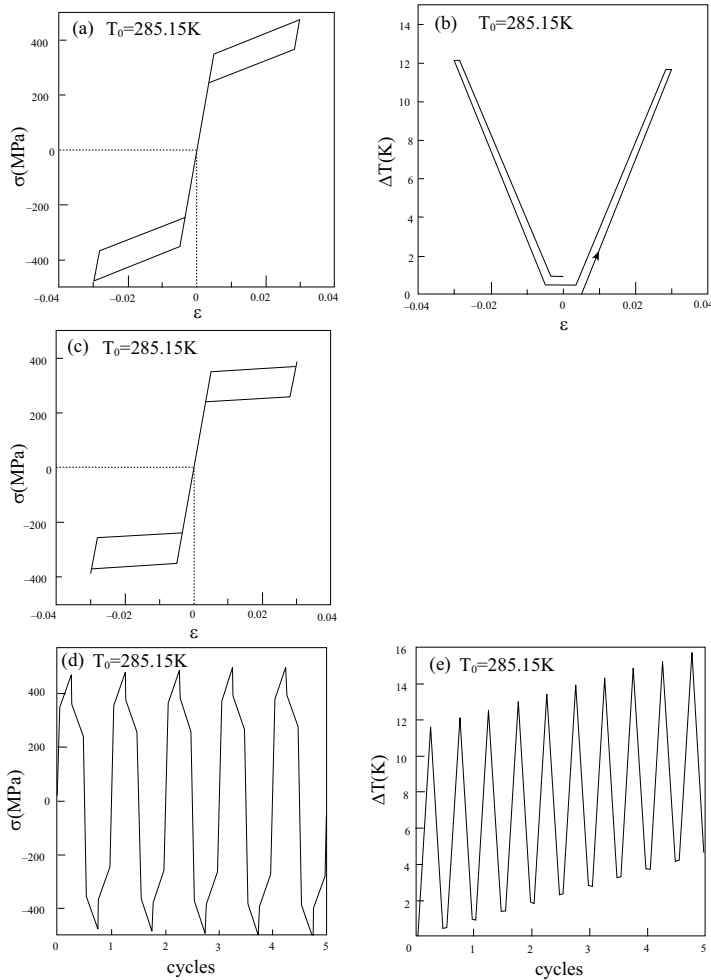


Figure 3. (a) The uniaxial stress-strain response in one cycle of SMA and, (b) the corresponding induced temperature deviation. (c) The corresponding uniaxial stress-strain response of SMA when the TMC is neglected. (d) The uniaxial stress-strain response in five cycles of SMA and (e) the corresponding induced temperature deviation. In all cases the reference temperature is $T_0 = 285.15$ K.

is a residual increase in the temperature (about 1 K) upon a complete uniaxial stress loading-unloading cycle of the homogeneous SMA material (where neither convection nor adiabatic conditions exist). It should be noted that the effect of the TMC on the response of the SMA that is depicted in Figure 2(a) and 3(a), as compared to Figure 2(c) and 3(c), results from the induced temperatures that affect the phase transformation and not by the generated thermal strains. For the reference temperature $T_0 = 285.15$ K, for example, the transformation strain at $\epsilon = 3\%$ is equal to 0.023 whereas the corresponding thermal strain is 0.12×10^{-4} .

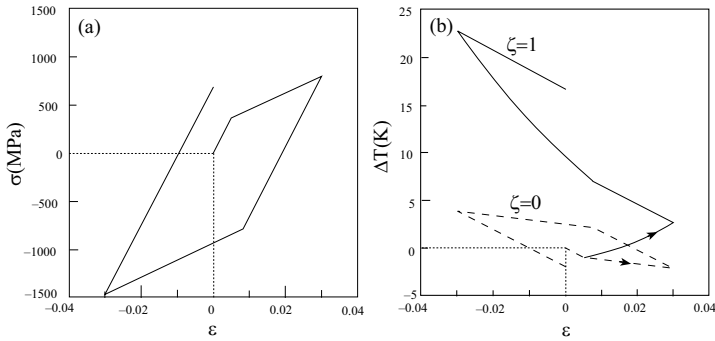


Figure 4. (a) The uniaxial stress-strain response in one cycle of the unreinforced aluminum and, (b) the resulting induced temperature deviation when $\zeta = 1$ and 0 in Equation (7).

Let us investigate the behavior of the SMA material that is subjected to a uniaxial stress cyclic loading. To this end, the SMA fiber at reference temperatures $T_0 = 253.15$ K and 285.15 K is subjected to five cycles of strain loading-unloading, and the resulting stress response and induced temperature are shown in Figure 2(d, e) and Figure 3(d, e). The stress shows a repetitive behavior but the continuously rising heat generation can be clearly observed.

4.2. SMA/aluminum composite. In order to investigate the behavior of the elastoplastic work-hardening aluminum matrix that has been characterized in Table 2, the uniaxial stress response of the (unreinforced) material to a cyclic loading is shown in Figure 4(a). The thermomechanical coupling coefficient δ that is given by Equation (22) is: $\delta = 0.027$. Therefore it is instructive to exhibit the induced temperature deviation during this cyclic loading in two different cases. To this end, Figure 4(b) shows the induced temperature when in Equation (7) $\zeta = 1$ and $\zeta = 0$. In the first case full TMC is taken into account, while in the second case the heat generated by the rate of plastic work \dot{W}_I is neglected while retaining the coupling caused by the term $3T K\alpha\dot{\theta}$ in this equation (which is accounted for by the coupling coefficient δ). Figure 4(b) clearly shows that the heat generated by the rate of plastic work is predominant. Except in Figure 4(b), ζ is taken in all cases to be equal to 1. The effect of TMC on the stress-strain response is negligibly small. Indeed, under a uniaxial stress loading at a strain of $\epsilon = 3\%$, the resulting inelastic and thermal strains are given by 0.019 and 0.56×10^{-4} , respectively.

Let us consider presently a composite in which the aluminum matrix is reinforced by SMA fibers that are oriented in the 1-direction. Figures 5 and 6 show the average uniaxial stress response $\bar{\sigma}_{11}$ to a cyclic loading of the composite in the axial direction and the resulting induced global temperature deviations $\Delta \bar{T}$ at two reference temperatures:

$$T_0 = 253.15 \text{ K} \quad \text{and} \quad 285.15 \text{ K}.$$

Although the curves in these figures appear to be quite similar, some differences can be detected which shows the effects of the SMA behavior at these two different reference temperatures. A comparison of these figures with the response of the unreinforced aluminum (that has been exhibited in Figure 4) provides further indications about the influence of the SMA fibers. The unreinforced aluminum is

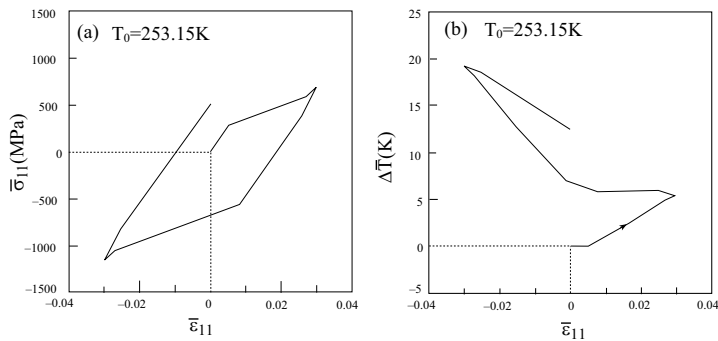


Figure 5. (a) The uniaxial stress-strain response in one cycle of the SMA/aluminum composite loaded in the fibers direction and, (b) the resulting induced average temperature deviation at a reference temperature $T_0 = 253.15\text{ K}$.

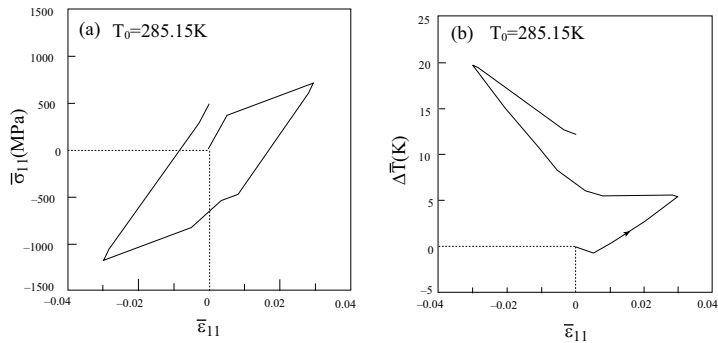


Figure 6. (a) The uniaxial stress-strain response in one cycle of the SMA/aluminum composite loaded in the fibers direction and, (b) the resulting induced average temperature deviation at a reference temperature $T_0 = 285.15\text{ K}$.

modeled as an elastic-plastic material with linear hardening, see Figure 4(a). A comparison of Figure 4(a) with Figure 5(a) and 6(a) shows that due to the existence of the SMA fibers, the linear hardening behavior is lost. Here too, just like the unreinforced aluminum, the effect of the TMC on the global stress-strain response of the SMA/aluminum composite is negligible.

It is interesting that the maximum induced temperature by the TMC in the unreinforced aluminum is greater than that obtained in the SMA/aluminum composite. This observation can be explained by the fact that the maximum temperature generated in the monolithic SMA is about 12 K (see Figure 2(b) and 3(b)), while in the monolithic aluminum it is about 23 K (see Figure 4(b)). The reinforcement by SMA fibers results in a decrease of the dominant effect of the aluminum which decreases the global temperature that is generated in the composite by the TMC.

The Young's moduli of the SMA fibers and the aluminum matrix are quite close to each other (70 MPa and 72.4 MPa, respectively). Consequently the response of the SMA/aluminum in the transverse 2-direction is quite similar to its response in the axial direction (shown in Figures 5 and 6).

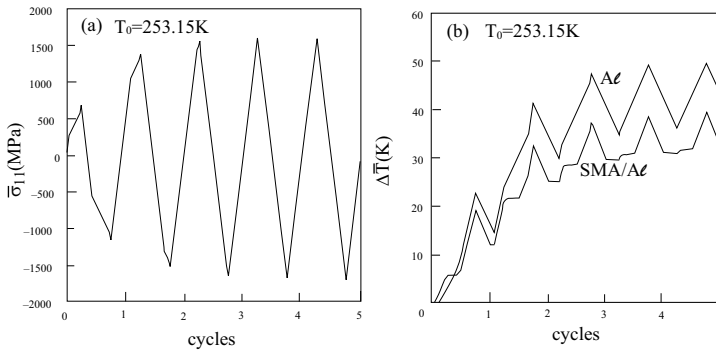


Figure 7. (a) The uniaxial response of the SMA/aluminum composite in 5 cycles loaded in the fibers direction and, (b) the resulting induced average temperature deviation at a reference temperature $T_0 = 253.15$ K. Also shown is the corresponding induced temperature deviation in the unreinforced aluminum.

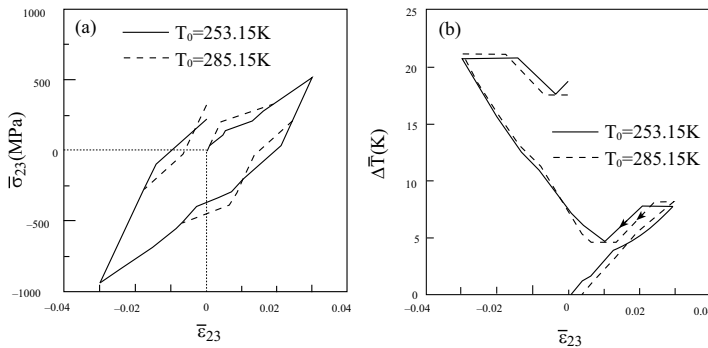


Figure 8. (a) The transverse shear stress-strain response in one cycle of the SMA/aluminum composite and, (b) the resulting induced average temperature deviation at reference temperatures: $T_0 = 253.15$ K and 285.15 K.

A further investigation of the induced temperature due to the two-way TMC can be performed by subjecting the SMA/aluminum composite to 5 cycles of uniaxial stress loading-unloading in the fibers direction at a reference temperature $T_0 = 253.15$ K. The resulting average axial stress response of the composite and the induced average temperature deviation are shown in Figure 7. The corresponding response to 5 cyclic loadings of the unreinforced aluminum matrix is quite similar (but with higher amplitude) to the composite response that is exhibited in Figure 7(a) and is not shown. The induced temperature of the unreinforced aluminum, on the other hand, is shown in Figure 7(b). Figure 7(b) reveals, as expected, the effect of TMC caused by the inelastic effects that appear in Equation (5) for the SMA fibers and Equation (7) for the aluminum. The latter effect appears to be predominant.

As a final illustration of the TMC effects in SMA/aluminum, we consider a cyclic transverse shear loading of the SMA/aluminum composite. Here average transverse shear stress-strain responses $\bar{\sigma}_{23} - \bar{\epsilon}_{23}$

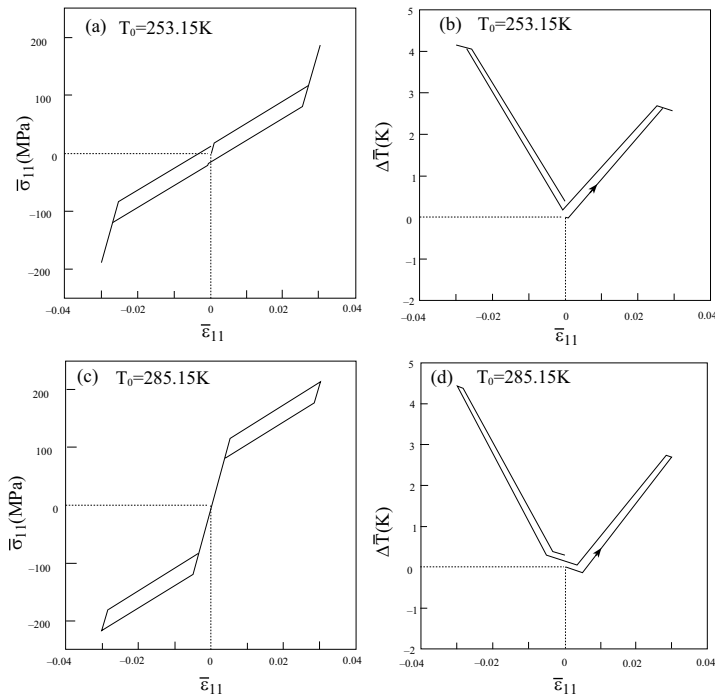


Figure 9. (a) The uniaxial stress-strain response in one cycle of the SMA/epoxy composite loaded in the fibers direction and, (b) the resulting induced average temperature deviation at a reference temperature $T_0 = 253.15\text{ K}$. (c) The uniaxial stress-strain response in one cycle of the SMA/epoxy composite loaded in the fibers direction and, (d) the resulting induced average temperature deviation at a reference temperature $T_0 = 285.15\text{ K}$.

of the composite at two reference temperatures:

$$T_0 = 253.15\text{ K} \quad \text{and} \quad 285.15\text{ K}$$

are shown in Figure 8. In addition, the resulting induced global temperature deviations $\Delta\bar{T}$ due to the TMC effects are also compared. Here too, the induced temperature is generated mainly by the rate of plastic work of the aluminum matrix. It should be noted that under a pure shear loading, the TMCs which cause the generation of temperatures in the monolithic SMA and the unreinforced aluminum are due to the first terms that represent the inelastic effects in the right side of Equation (5) and (7). The second term $3 T K\alpha\dot{\theta}$ in both equations vanishes in this case.

4.3. SMA/epoxy composite. Consider the epoxy matrix whose material parameters are given in Table 3. Its thermomechanical coupling coefficient is quite small: $\delta = 0.016$. Consequently, due to the absence of inelastic effects in this polymer, it is expected that the effect of TMC will be weak and the induced temperature deviation will not be significant. In Figure 9, the uniaxial response to a cyclic loading in the

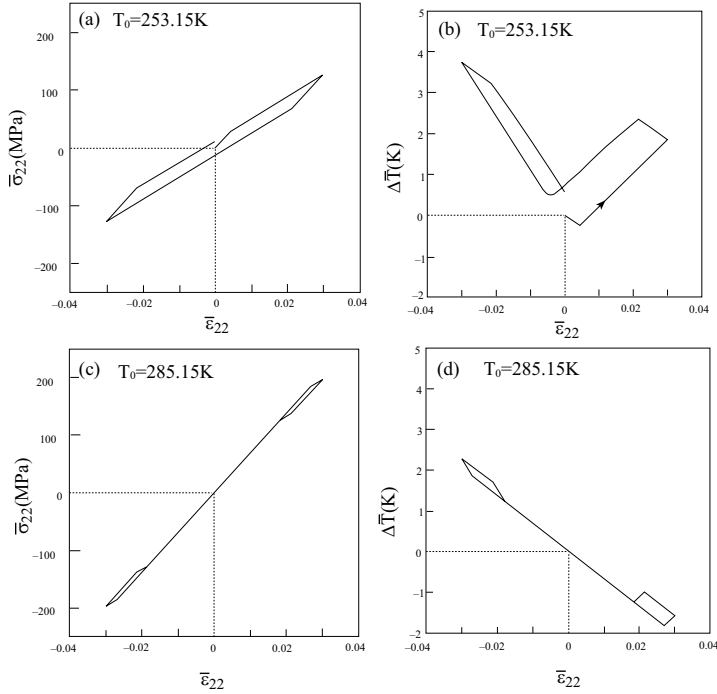


Figure 10. (a) The uniaxial stress-strain response in one cycle of the SMA/epoxy composite loaded in the perpendicular direction of to the fibers and, (b) the resulting induced average temperature deviation at a reference temperature $T_0 = 253.15\text{ K}$. (c) The uniaxial stress-strain response in one cycle of the SMA/epoxy composite loaded in the perpendicular direction of to the fibers and, (d) the resulting induced average temperature deviation at a reference temperature $T_0 = 285.15\text{ K}$.

fibers' direction of SMA/epoxy composite is shown at two reference temperatures:

$$T_0 = 253.15\text{ K} \quad \text{and} \quad T_0 = 285.15\text{ K}.$$

Also shown are the resulting average temperatures that are generated due to the TMC effect. The figure shows that quite different stress-strain behaviors are obtained by loading-unloading of the composite at the two reference temperatures, but the induced temperatures are very similar. The Young's moduli of the SMA fiber and epoxy matrix are quite different (70 GPa and 3.45 GPa , respectively). Thus the uniaxial responses of the composite to loading in the axial direction (that is, parallel to the fibers) and transverse direction (that is, perpendicular to the fibers) should be quite different. This difference can be observed by comparing Figure 9 with Figure 10 which exhibits the transverse response of the SMA/epoxy composite at the same reference temperatures.

A careful check of the temperatures that are generated by a uniaxial stress loading-unloading of the pure SMA, Figures 2(b) and 3(b), reveal that there is asymmetry that can be clearly observed at the final strain of $\epsilon = \pm 3\%$ at which the temperature deviations ΔT are not equal. The combined effects of the (asymmetric) temperature generated by loading-unloading cycle of the SMA fibers and the (symmetric)

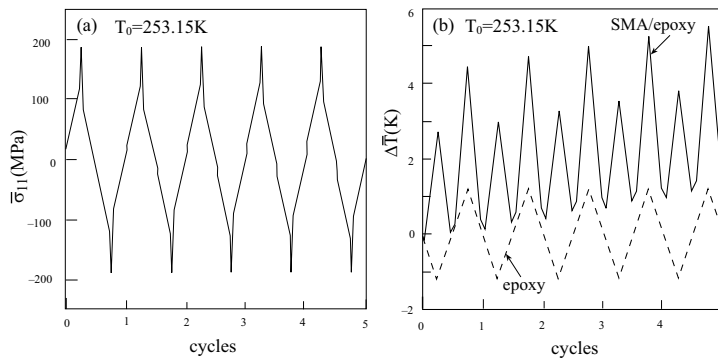


Figure 11. (a) The uniaxial response of the SMA/epoxy composite in 5 cycles loaded in the fibers direction and, (b) the resulting induced average temperature deviation at a reference temperature $T_0 = 253.15 \text{ K}$. Also shown is the corresponding induced temperature deviation in the unreinforced epoxy.

temperature generated in the epoxy matrix that are shown in Figures 9(b), 9(d), 10(b) and 10(d) at a finer scale, exhibit the resulting asymmetries in the global induced temperatures of the SMA/epoxy composite.

As a final illustration of the SMA/epoxy composite behavior, we present in Figure 11 the response of the composite to 5 cycles of uniaxial stress loading in the fibers direction at a reference temperature

$$T_0 = 253.15 \text{ K}.$$

Of particular interest is the uniform periodic temperature that is induced in the unreinforced epoxy caused by the TMC (in the absence of any irreversible effects). This is in contrast to the nonuniform and continuously increasing temperature in the monolithic SMA fiber that was shown in Figure 2(e) which is caused by the irreversible effects in this material. As a result, the induced temperature $\Delta \bar{T}$ caused by the TMC effects in the SMA/epoxy composite exhibits an irregular pattern as shown in Figure 11(b).

We conclude the paper by mentioning that by subjecting the SMA/epoxy composite to a transverse shear loading, the amount of the induced temperature is very small implying that the effect of TMC is negligibly small in this case.

5. Conclusions

A micromechanical model which can predict the behavior of multiphase inelastic composites with one-way TMC has been generalized to incorporate two-way TMC effects in the presence of SMA phases. The generalization results in coupled mechanical and energy equations in which the temperature is induced in the phases as a result of the application of far field mechanical loadings. Overall macroscopic thermoelastic constitutive equations of composites with two-way TMC have been established. They represent the global behavior of the SMA fiber composite at every increment of loading. The results show that two-way TMC must be taken into account when dealing with SMA/metallic composites, and that it has a minor effect in SMA/polymeric composites. This is due to the inelastic effects that generate heat in the metallic phase in addition to the portion of heat obtained from the volumetric strain rate.

Damage effects were not taken into account in the present modeling of the monolithic SMA material or in the SMA composite. Considerations of such effects is a subject for future research.

The present micromechanical model can be employed to investigate the behavior of SMA composite structures with two-way TMC. In particular, the induced temperatures that are caused by bending, buckling, postbuckling and vibrations of a SMA composite structure can be determined by employing a micro-macro-structural analysis according to which the global constitutive equations that are obtained from the proposed model are applied at every point of the structure.

Acknowledgments

The first author gratefully acknowledges the support of the Diane and Arthur Belfer chair of Mechanics and Biomechanics. Special thanks go to Dr. Rivka Gilat, JAS College, for fruitful discussions.

References

- [Aboudi 2004] J. Aboudi, “The generalized method of cells and high-fidelity generalized method of cells micromechanical models—a review”, *Mech. Adv. Mater. Struct.* **11** (2004), 329–366.
- [Aboudi 2005] J. Aboudi, “[Micromechanically established constitutive equations for multiphase materials with viscoelastic-viscoplastic phases](#)”, *Mech. Time-Depend. Mat.* **9**:2-3 (2005), 121–145.
- [Aboudi et al. 2002] J. Aboudi, M.-J. Pindera, and S. M. Arnold, “[High-fidelity generalization method of cells for inelastic periodic multiphase materials](#)”, NASA, Houston, 2002, Available at <http://gltrs.grc.nasa.gov/citations/all/tm-2002-211469.html>.
- [Aboudi et al. 2003] J. Aboudi, M.-J. Pindera, and S. M. Arnold, “[Higher-order theory for periodic multiphase materials with inelastic phases](#)”, *Int. J. Plasticity* **19**:6 (2003), 805–847.
- [Allen 1991] D. H. Allen, “Thermo-mechanical coupling in inelastic solids”, *Appl. Mech. Rev.* **44** (1991), 361–373.
- [Auricchio and Petrini 2002] F. Auricchio and L. Petrini, “[Improvements and algorithmical considerations on a recent three-dimensional model describing stress-induced solid phase transformations](#)”, *Int. J. Numer. Meth. Eng.* **55**:11 (2002), 1255–1284.
- [Auricchio and Petrini 2004a] F. Auricchio and L. Petrini, “[A three-dimensional model describing stress-temperature induced solid phase transformations: solution algorithm and boundary value problems](#)”, *Int. J. Numer. Meth. Eng.* **61**:6 (2004), 807–836.
- [Auricchio and Petrini 2004b] F. Auricchio and L. Petrini, “[A three-dimensional model describing stress-temperature induced solid phase transformations: thermomechanical coupling and hybrid composite applications](#)”, *Int. J. Numer. Meth. Eng.* **61**:5 (2004), 716–737.
- [Bednarczyk and Arnold 2002] B. A. Bednarczyk and S. M. Arnold, “[MAC/GMC 4.0 user’s manual](#)”, NASA, Houston, 2002, Available at <http://gltrs.grc.nasa.gov/cgi-bin/GLTRS/browse.pl?2002/TM-2002-212077-VOL3.%html>.
- [Bednarczyk et al. 2004] B. A. Bednarczyk, S. M. Arnold, J. Aboudi, and M.-J. Pindera, “[Local field effects in titanium matrix composites subjected to fiber-matrix debonding](#)”, *Int. J. Plasticity* **20**:8-9 (2004), 1707–1737.
- [Boyd and Lagoudas 1994] J. G. Boyd and D. C. Lagoudas, “[Thermomechanical response of shape memory composites](#)”, *J. Intel. Mat. Syst. Struct.* **5**:3 (1994), 333–346.
- [Carvelli and Taliercio 1999] V. Carvelli and A. Taliercio, “[A micromechanical model for the analysis of unidirectional elastoplastic composites subjected to 3D stresses](#)”, *Mech. Res. Commun.* **26**:5 (1999), 547–553.
- [Gilat and Aboudi 2004] R. Gilat and J. Aboudi, “[Dynamic response of active composite plates: shape memory alloy fibers in polymeric/metallic matrices](#)”, *Int. J. Solids Struct.* **41**:20 (2004), 5717–5731.
- [Gilat and Aboudi 2006] R. Gilat and J. Aboudi, “[Thermal buckling of activated shape memory reinforced laminated plates](#)”, *Smart Mater. Struct.* **15** (2006), 829–838.
- [Hunter 1983] S. C. Hunter, *Mechanics of continuous media*, 2nd ed. ed., Ellis Horwood Ltd, Chichester, 1983.
- [Kawai 2000] M. Kawai, “[Effects of matrix inelasticity on the overall hysteretic behavior of TiNi-SMA fiber composites](#)”, *Int. J. Plasticity* **16**:3-4 (2000), 263–282.

- [Kawai et al. 1999] M. Kawai, H. Ogawa, V. Baburaj, and T. Koga, “[Micromechanical analysis for hysteretic behavior of unidirectional TiNi SMA fiber composites](#)”, *J. Intel. Mat. Syst. Struct.* **10**:1 (1999), 14–28.
- [Marfia 2005] S. Marfia, “[Micro-macro analysis of shape memory alloy composites](#)”, *Int. J. Solids Struct.* **42**:13 (2005), 3677–3699.
- [Mitchell and Griffiths 1980] A. R. Mitchell and D. F. Griffiths, *The finite difference method in partial differential equations*, John Wiley, Chichester, 1980.
- [Simo and Hughes 1998] J. C. Simo and T. J. R. Hughes, *Computational inelasticity*, Springer, New York, 1998.
- [Song et al. 1999] G. Q. Song, Q. P. Sun, and M. Cherkaoui, “Role of microstructures in the thermomechanical behavior of SMA composites”, *J. Eng. Mater. Tech.* **121** (1999), 86–92.
- [Souza et al. 1998] A. C. Souza, E. N. Mamiya, and N. Zouain, “[Three-dimensional model for solids undergoing stress-induced phase transformations](#)”, *Eur. J. Mech. A/Solids* **17**:5 (1998), 789–806.
- [Williams and Aboudi 1999] T. O. Williams and J. Aboudi, “[A fully coupled thermomechanical micromechanics model](#)”, *J. Therm. Stresses* **22**:9 (1999), 841–873.

Received 13 Feb 2006. Accepted 5 Apr 2006.

JACOB ABOUDI: aboudi@eng.tau.ac.il

Department of Solid Mechanics, Materials and Systems, Faculty of Engineering, Tel Aviv University, Ramat Aviv 69978, Israel

<http://www.eng.tau.ac.il/~aboudi/>

YUVAL FREED: yuval@eng.tau.ac.il

Department of Solid Mechanics, Materials and Systems, Faculty of Engineering, Tel Aviv University, Ramat Aviv 69978, Israel

JOURNAL OF MECHANICS OF MATERIALS AND STRUCTURES

<http://www.jomms.org>

EDITOR-IN-CHIEF Charles R. Steele

ASSOCIATE EDITOR Marie-Louise Steele
Division of Mechanics and Computation
Stanford University
Stanford, CA 94305
USA

SENIOR CONSULTING EDITOR Georg Herrmann
Ortstrasse 7
CH-7270 Davos Platz
Switzerland

BOARD OF EDITORS

D. BIGONI University of Trento, Italy
H. D. BUI École Polytechnique, France
J. P. CARTER University of Sydney, Australia
R. M. CHRISTENSEN Stanford University, U.S.A.
G. M. L. GLADWELL University of Waterloo, Canada
D. H. HODGES Georgia Institute of Technology, U.S.A.
J. HUTCHINSON Harvard University, U.S.A.
C. HWU National Cheng Kung University, R.O. China
IWONA JASIUŁ University of Illinois at Urbana-Champaign
B. L. KARIHALOO University of Wales, U.K.
Y. Y. KIM Seoul National University, Republic of Korea
Z. MROZ Academy of Science, Poland
D. PAMPLONA Universidade Católica do Rio de Janeiro, Brazil
M. B. RUBIN Technion, Haifa, Israel
Y. SHINDO Tohoku University, Japan
A. N. SHUPIKOV Ukrainian Academy of Sciences, Ukraine
T. TARNAI University Budapest, Hungary
F. Y. M. WAN University of California, Irvine, U.S.A.
P. WRIGGERS Universität Hannover, Germany
W. YANG Tsinghua University, P.R. China
F. ZIEGLER Technische Universität Wien, Austria

PRODUCTION


PAULO NEY DE SOUZA Production Manager
SHEILA NEWBERY Senior Production Editor
SILVIO LEVY Scientific Editor

See inside back cover or <http://www.jomms.org> for submission guidelines.

JoMMS (ISSN 1559-3959) is published in 10 issues a year. The subscription price for 2006 is US \$400/year for the electronic version, and \$500/year for print and electronic. Subscriptions, requests for back issues, and changes of address should be sent to Mathematical Sciences Publishers, Department of Mathematics, University of California, Berkeley, CA 94720-3840.

JoMMS peer-review and production is managed by EditFLOW™ from Mathematical Sciences Publishers.

PUBLISHED BY

 **mathematical sciences publishers**
<http://www.mathscipub.org>

A NON-PROFIT CORPORATION

Typeset in L^AT_EX

©Copyright 2006. Journal of Mechanics of Materials and Structures. All rights reserved.

Journal of Mechanics of Materials and Structures

Volume 1, Nº 5 May 2006

Plane harmonic elasto-thermodiffusive waves in semiconductor materials	JAGAN NATH SHARMA and NAVEEN THAKUR	813
Thermomechanical formulation of strain gradient plasticity for geomaterials	JIDONG ZHAO, DAICHAO SHENG and IAN F. COLLINS	837
The effect of contact conditions and material properties on elastic-plastic spherical contact	VICTOR BRIZMER, YUVAL ZAIT, YURI KLIGERMAN and IZHAK ETSION	865
Asymptotic fields at frictionless and frictional cohesive crack tips in quasibrittle materials	QIZHI XIAO and BHUSHAN LAL KARIHALOO	881
Analysis of electromechanical buckling of a prestressed microbeam that is bonded to an elastic foundation	DAVID ELATA and SAMY ABU-SALIH	911
On uniqueness in the affine boundary value problem of the nonlinear elastic dielectric	R. J. KNOPS and C. TRIMARCO	925
Two-way thermomechanically coupled micromechanical analysis of shape memory alloy composites	JACOB ABOUDI and YUVAL FREED	937